Case Studies in Thermal Engineering 24 (2021) 100847

Contents lists available at ScienceDirect

Case Studies in Thermal Engineering

journal homepage: http://www.elsevier.com/locate/csite

Combustion and fire safety of energy conservation materials in building vertical channel: Effects of structure factor and coverage rate

Weiguang An [a,b,c,*], Song Li [a,b], Xiangwei Yin [a,b], Lujun Peng [a,b]

[a] Jiangsu Key Laboratory of Fire Safety in Urban Underground Space (China University of Mining and Technology), Xuzhou, 221116, China
[b] Key Laboratory of Gas and Fire Control for Coal Mines (China University of Mining and Technology), Ministry of Education, Xuzhou, 221116, China
[c] State Key Laboratory of Coal Resources and Safe Mining, China University of Mining and Technology, No. 1 University Road, Xuzhou, Jiangsu, 221116, China

ARTICLE INFO

Keywords:
Energy conservation
Thermal insulation materials
Fire safety
Combustion
Flame spread
Heat transfer

ABSTRACT

Experimental study on combustion and fire safety of energy conservation materials (extruded polystyrene, i.e., XPS) in vertical channel with front openings of building façade is conducted, and effects of channel structure factor (α) and curtain wall coverage rate (β) are revealed. The XPS flame in the vertical channel is turbulent. There is a correlation between the flame height and pyrolysis length: $x_f = mx_p^n$, where m and n vary with the change in structure factor and coverage rate. Upward flame spread rate decreases first and then increases as β rises. When $0 \leq \beta < 0.2$, the restraining effect of vertical channel on air entrainment dominates, while for $0.2 \leq \beta \leq 0.8$, the heat feedback from curtain wall dominates. When $\beta = 0$, the influence of α on flame spread rate is not significant. The flame spread rate increases with increasing α when $0.2 \leq \beta \leq 0.8$. A model is established to predict the flame spread rate under different coverage rates and structure factors. Compared with experimental results, the prediction error is smaller than 10%. Larger values of flame height and flame spread rate correspond to higher fire hazard. This work is beneficial for fire safety assessment of building thermal insulation materials and optimal design of energy-saving curtain wall.

1. Introduction

Building energy consumption accounts a large proportion of total energy consumption in global. Thus building energy conservation is vital for social sustainable development. New building materials and building structures are applied to achieve better energy conservation, ignoring the safety at times. The energy conservation and safety are contradictory under certain conditions. It is necessary to search the balance between the energy conservation and safety.

Thermal insulation materials, including extruded polystyrene (XPS), molded polystyrene (EPS), polyurethane (PU) et al., are typical energy conservation materials using on the building façade [1,2]. However, these materials introduce high fire hazard to buildings. The typical example is the Grenfell Tower fire occurred in London in 2017, leading to at least 72 deaths. Therefore, both the

* Corresponding author. Jiangsu Key Laboratory of Fire Safety in Urban Underground Space (China University of Mining and Technology), Xuzhou, 221116, China.
E-mail address: weiguang@cumt.edu.cn (W. An).

https://doi.org/10.1016/j.csite.2021.100847
Received 14 August 2020; Received in revised form 21 December 2020; Accepted 11 January 2021
Available online 16 January 2021

fire safety and energy conservation should be considered when the properties of thermal insulation materials are evaluated. In addition, curtain walls are often installed over the facade of modern buildings, and a vertical channel is formed between the curtain wall and the façade (Fig. 1 (a) and (b)). The purpose of installing curtain wall is to optimize lighting, save energy, and improve the beauty of the building. However, the fire safety of thermal insulation materials will be significantly influenced by the vertical channel (Fig. 1 (c)). For example, flame spread is promoted by the vertical channel formed by the curtain wall and façade during the XPS fire of CCTV building (February 9, 2009) in China. Therefore, it is necessary to investigate the combustion and fire safety of energy conservation materials in vertical channel of building facade.

The combustion and fire safety of thermal insulation materials have attracted some attention of researchers. Zhou et al. [3,4] studied the upward flame spread over rigid polyurethane foams under the coupling effect of inclination angle and ambient pressure. Their experimental results showed that the flame changed from laminar flow to turbulent flow with the increasing inclination angle. Investigating the upward flame spread over discrete polystyrene (PS) with different fuel coverages, Wang et al. [5] found that the average flame spread rate was positively correlated with the fuel coverage, while Meng et al. [1] indicated that the average flame height first decreased and then increased as the fuel coverage rises. In addition, melting and dripping during the XPS combustion would intensify the heat transfer, leading to acceleration of flame spread [6,7]. Some experiments and numerical simulations have been performed to study combustion and flame spread behaviors of solids under the effects of vertical channels. An et al. [8] conducted both experimental and theoretical study on upward flame spread over PMMA (polymethyl methacrylate) plate under different U-shaped structure factors, and two models were established to predict flame spread rates with different structure factors for laminar and turbulent flame, respectively. Avinash et al. [9] studied the impact of vertical channels formed by multiple fuel sheets on downward flame spread, and found that oxygen supply and heat transfer jointly controlled the flame spread rate. Matsuoka et al. [10] investigated the influence of the geometry of channel on the flame spread rate of thin materials. The experimental results revealed that the flame spread rate increased first and then decreased with the increasing channel height. Comas et al. [11] found that the frontal-enclosed vertical channel enhanced the upward airflow velocity, which leaded to the increase in the flame spread rate. When the oxygen concentration was sufficiently high, a concurrent premixed flame with a higher spread rate was observed. An et al. [12] investigated the influence of frontal-enclosed vertical channel on downward flame spread over XPS, and found that the flame spread rate first increased and then decreased with the increasing structure factor, i.e., the ratio of width to length of the channel cross section. Relevant heat transfer models have been established to predict heat feedback on the surface of the preheating zone. Conducting a series of large-scale experiments, Yan et al. [13] found that the larger the structure factor of the concave channel, the higher the flame. The maximum flame height slightly increased with an increase in the structure factor. Li et al. [14] indicated that the flame spread in a concave channel accelerated over time. Enhanced by the chimney effect, both the flame spread rate and mass loss rate increased with the increasing structure factor. Zhu et al. [15] indicated that as the spacing of frontal-enclosed vertical channel increases, the downward flame spread rate of PMMA increased first and then decreased. Gao et al. [16] found the flame spread rate was proportional to the flame width under the influence of frontal-enclosed vertical channel.

The above researches mainly focus on the impact of channel structure factor, and the vertical channels are mainly concave channel and frontal-enclosed channel. There are few works concerning combustion and fire safety of energy conservation materials in a frontal-open channel with different curtain wall coverage rates (i.e., the ratio of curtain wall coverage area to the total front area of vertical channel). Moreover, the coupling effects of structure factor and coverage rate have not been revealed. Therefore, this paper investigates effects of structure factor and coverage rate on combustion and fire safety of energy conservation materials in frontal-open vertical channel of building facade.

2. Experimental device, material and methods

The experimental device is shown in Fig. 2. The vertical channel consisted of a backwall, two sidewalls and a curtain wall, among

Fig. 1. (a) Frontal-enclosed vertical channel; (b) frontal-open vertical channel; (c) thermal insulation material fire in a concave vertical channel.

which the backwall and the sidewalls were made of cement board with low thermal conductivity and high temperature resistance. In order to facilitate the observation of the flame characteristics from the front of the curtain wall, the curtain wall was made of PMMA (Polymethyl Methacrylate) with a size of 10 cm × 10 cm × 0.3 cm (length × width × thickness). The typical thermal insulation material, i.e., extruded polystyrene (XPS) was selected as experimental material. The thermal parameters of XPS samples are shown in Table 1 [1]. A non-flame-retardant XPS sample (100 cm long, 10 cm wide, and 3 cm thick) was nailed to the backwall. The back of each XPS sample was wrapped with aluminum foil to prevent molten XPS from flowing onto the backwall. There may be small interspace between the back of XPS sample and the backwall since the surfaces of both XPS sample and backwall were not absolutely flat. If the aluminum foil was not used, the back of the XPS sample may also burn. The aluminum foil could eliminate above mentioned interspace and prevent the burning of XPS back, which is more in line with the actual application scenario of XPS materials. The bottom of XPS samples were 20 cm away from the ground, which reduced the effect of the ground on the air entrainment.

A CCD camera was fixed in front of the curtain wall to record the flame spread behavior. The performance parameters of the camera are shown in Table 2 [17]. In this paper, K-type thermocouples were employed to measure the flame spread rate. The diameter of the thermocouple was 0.5 mm, the response time was 0.3s, the measurement range was 0–1000 °C, and the accuracy was ±2.2 °C. The thermocouples were embedded into the XPS samples to monitor the changes in temperature. The insertion depth of the thermocouples was 1.5 cm. When the thermocouple temperature reached the pyrolysis temperature, the pyrolysis front was considered to spread to the position of the thermocouple, and thus the position of the pyrolysis front could be determined. Further, the flame spread rate and the pyrolysis length could be obtained. This method was also used in the previous study [18].

The experimental conditions are shown in Fig. 2 (a). The structure factor (α) was defined as the ratio of the length of the sidewall to the width of the material, i.e., $\alpha = W_{sw}/W$. The length of the sidewall was set as 10 cm, 12 cm, and 14 cm, respectively, thus the structure factors were 1.0, 1.2, and 1.4. Since the thickness of the PMMA sample is 3 cm, the distance between PMMA burning surface and curtain wall is 7 cm ($\alpha = 1.0$), 9 cm ($\alpha = 1.2$), and 11 cm ($\alpha = 1.4$), respectively. Curtain wall coverage rate (β) was defined as the ratio of curtain wall coverage area to the total front area of vertical channel, i.e., $\beta = (S_1 + \ldots + S_n)/S$. The coverage rates were set as 0, 0.2, 0.4, 0.6, and 0.8, respectively. The environmental conditions of the experiments are as follows: the atmospheric pressure was 100.07 kPa, the ambient temperature was 30 °C, and the humidity was 65%. The physical model of flame spread and heat transfer mode in the vertical channel is shown in Fig. 2 (c). Each test is repeated at least three times to reduce the experimental error.

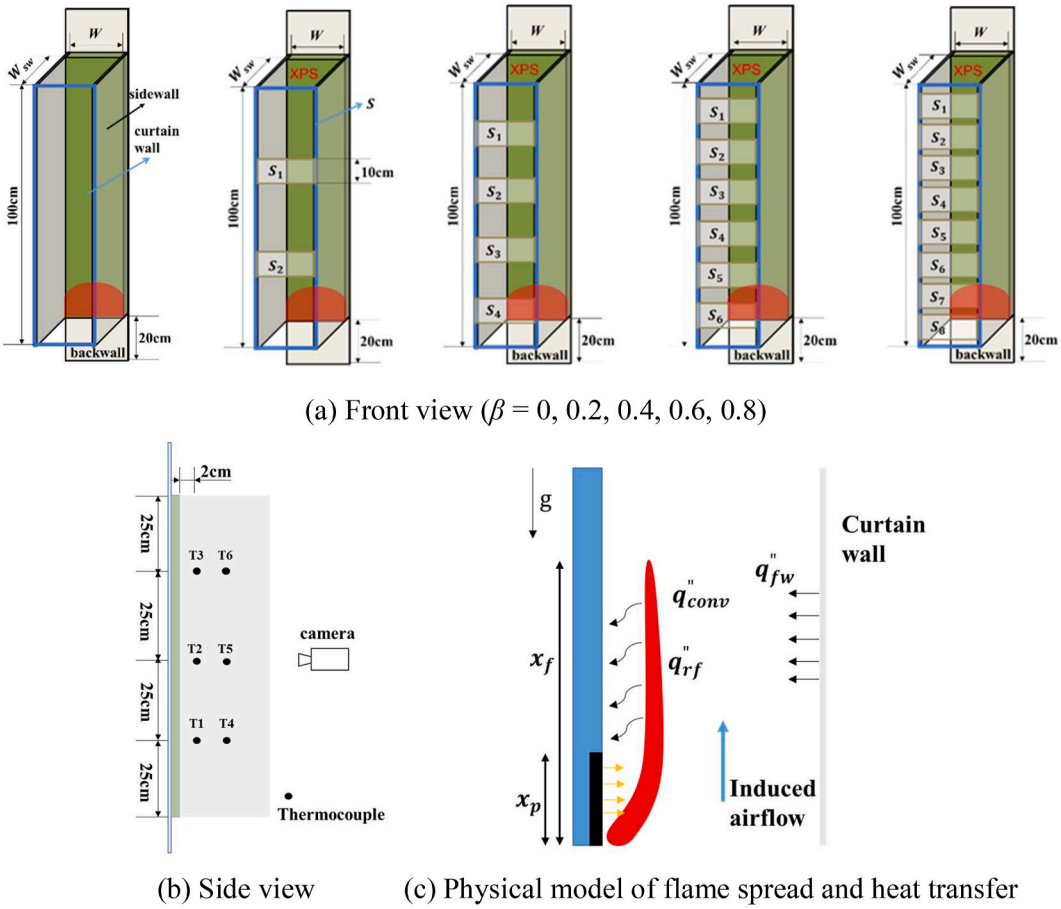

Fig. 2. Experimental device and conditions.

Table 1
Thermal parameters of XPS samples [1].

Materials	Thermal conductivity W/(m·K)	Pyrolysis temperature °C	Ignition temperature °C	Density g/cm^3	Specific heat kJ/(kg·K)
XPS	0.029	350~400	427.2	34	1210

Table 2
Performance parameters of the digital camera.

Performance parameter	Parameter value
Type	SONY HDR-CX450
Frame rate	25 fps
Resolution ratio	1920 × 1080
Maximum aperture	F1.8-F4.0
Actual focal length	f = 1.9–57.0 mm
Video format	AVCHD

3. Results and discussion

In this work, results concerning XPS combustion characteristics including the temperature distribution, flame height, pyrolysis length and flame spread rate were measured and discussed. The flame height is defined as the distance from the bottom of the visible flame to its top, while the pyrolysis length is the distance from the burnout front to the pyrolysis front [16,17]. Commonly larger values of flame height and flame spread rate correspond to higher fire hazard. The fire safety of XPS in vertical channel under different structure factors and coverage rates were evaluated.

3.1. Temperature distribution

The temperature distribution in the vertical channel was measured with thermocouples, whose location is shown in Fig. 3. The maximum temperature of each thermocouple was recorded. Further, the average values of maximum temperatures of three thermocouples in the center of the vertical channel and those 2 cm away from XPS surface are calculated, respectively. The results are presented in Fig. 3. The average value of maximum temperatures 2 cm away from XPS surface ($\overline{T}_{max-2}$)is much higher than that in the center of the vertical channel ($\overline{T}_{max-c}$). The reason is that the thermocouples 2 cm away from the XPS surface is closer to the flame, receiving more convective and radiative heat feedback from the flame. When the structure factor is 1.0, $\overline{T}_{max-2}$ decreases with the increase of coverage rate. When the structure factors are 1.2 and 1.4, with the increase of the coverage rate, the variation of $\overline{T}_{max-2}$ is not significant. Ji et al. [19] proposed a formula for calculating the pressure difference between the channel inside and outside, i.e., $\Delta P = \rho_\infty T_\infty \left(\frac{1}{T_\infty} - \frac{1}{T_v}\right) gh$, where ρ_∞, T_∞, T_v and h denote the air density, the ambient temperature, the average value of maximum temperature in the center of the vertical channel and the height of the vertical channel, respectively. It is deduced from Ji's formula that the higher the temperature inside the channel, the larger the pressure difference, and thus the stronger the chimney effect. Therefore, it can be concluded from Fig. 3 that when the structural coefficient is 1.0, the intensity of the chimney effect decreases with

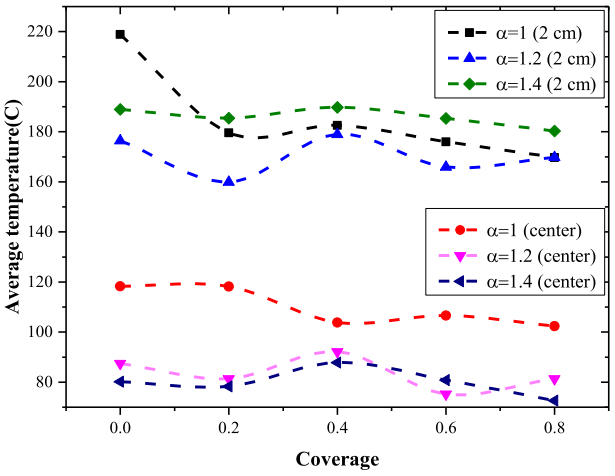

Fig. 3. The average value of maximum temperature inside the vertical channel under different structure factors and coverage rates.

the increase of the coverage rate. When the structural factors are 1.2 and 1.4, the coverage rate has no significant effect on the intensity of the chimney effect. In addition, with the increase of the coverage rate, the change in average value of maximum temperatures in the center of vertical channel is also not obvious.

When the coverage rate is unchanged, $\overline{T}_{max-2}$ first decreases and then increases with an increase in the structure factor. The reason is that with the increase of the structure factor, the restrict effect on the front air supply is more significant, resulting in insufficient oxygen supply and insufficient combustion, which inhibits temperature increase. On the other hand, the increase in the structure factor leads to the increase of channel space, and the entrained airflow is fully heated to accelerate combustion, which promotes the increase in temperature. The competition between above two factors leads to the non-linear change of $\overline{T}_{max-2}$. In addition, with the increase of the structure factor, the average value of maximum temperatures in the center of vertical channel gradually decreases. This could be attributed to the larger distance from the thermocouple to the flame under larger structure factor. The larger distance leads to less convective and radiant heat transfer from the flame to the thermocouple, and thus the temperature decreases.

3.2. Flame height and pyrolysis length

It can be seen from Fig. 2 (c) that after the material is ignited, the flame gradually stabilizes and spreads upward. The pyrolysis gas generated in the pyrolysis zone is ignited and then forms the flame. Therefore, there is a certain correlation between the pyrolysis length and the flame height [20]. The flame height is closely related with the flow state [21], and the natural convection on the vertical surface is often described using G_r[22],

$$Gr = \frac{g\beta_g (T_f - T_\infty) L^3 \rho_g^2}{\mu_g^2} \tag{1}$$

where T_f and T_∞ is the flame temperature and ambient temperature, g , β_g, ρ_g and μ_g denote the acceleration of gravity, expansion coefficient, air density and dynamic viscosity, respectively. L represents the characteristic length, which is 100 cm. In our experiment, the value of Gr is larger than 10^9, and thus the flame is turbulent.

The correlation between the flame height and pyrolysis length of upward flame spread is [23]:

$$x_f = m x_p^n \tag{2}$$

where x_f and x_p are the flame height and pyrolysis length, respectively. When the flame is laminar flow, n is 1, and when the flame is

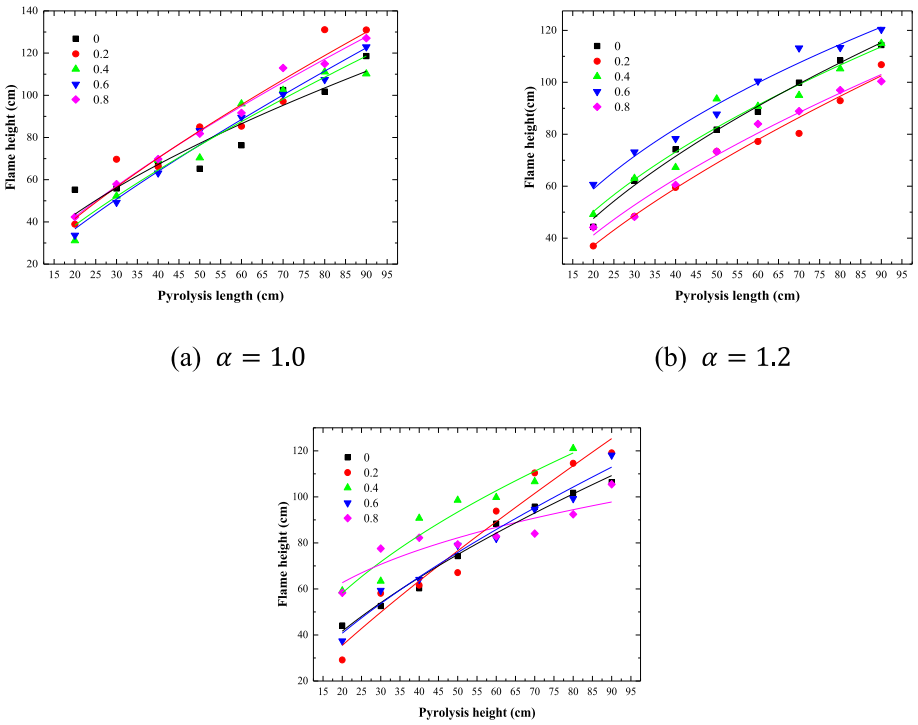

Fig. 4. The fitting curve concerning the flame height and pyrolysis length.

turbulent flow, n is 2/3.

The image processing method was used to obtain the flame height. The camera was employed to record the whole process of flame spread over the sample. These videos were converted into RGB images. Using a MATLAB program, each RGB image was converted into a binary image. Then the number of the binary image pixels with a value of 1 was counted and deemed as the flame zone. The length of the flame zone was the flame height. Moreover, the method to obtain the pyrolysis length has been explained in section 2. The experimental results of the flame height and pyrolysis length are shown in Fig. 4.

According to Eq. (2), non-linear curve fitting of the data concerning the flame height and pyrolysis length in Fig. 4 was conducted. Then the fitting values of m and n were obtained and shown in Table 3, where the value of n is close to 2/3. Thus, it can be judged that the flame in this experiment is closer to the turbulent state.

3.3. Flame spread rate

As shown in Fig. 2 (c), the flame spread behavior is closely related to the heat transfer and mass transfer between the gas phase flame and the solid phase combustibles [1,15,24]. As shown in Table 1, the thermal conductivity of XPS is 0.029 W/(m·K), which is very low. It is deduced that the heat conduction inside the XPS sample is little and can be ignored. Therefore, the flame spread behavior is mainly determined by the heat feedback from the flame to the virgin materials, and the radiative heat feedback from the curtain wall to the virgin materials. An et al. [18] established a model suitable for flame spread in a vertical channel based on the analysis of heat and mass transfer,

$$V_f \propto \dot{q}''_{concv} + \dot{q}''_{rf} + \dot{q}''_{fw} \tag{3}$$

where $\dot{q}''_{conv}$, $\dot{q}''_{rf}$ and $\dot{q}''_{fw}$ are convective heat flux, radiative heat flux of flame and radiative heat feedback of curtain wall, respectively.

In general, convective heat flux can be expressed as $\dot{q}''_{conv} = \frac{k_g u_\infty}{\alpha_g}(T_f - T_p)$, where k_g is the gas phase thermal conductivity, u_∞ is the induced airflow, α_g denotes the thermal diffusion coefficient, and T_p is the pyrolysis temperature. The convective heat flux is mainly determined by the flame temperature and the induced airflow velocity inside the channel [25]. Assuming that the flame temperature and pyrolysis temperature do not change with structure factor and coverage rate, it can be deduced that the chimney effect is weak, which means that the induced airflow velocity inside the channel is almost unchanged [16]. Therefore, the convective heat flux can be regarded as a fixed value. The radiative heat flux of the flame can be expressed as $\dot{q}''_{rf} = 0.9\sigma K_f \delta W(T_f^4 - T_p^4)$ [26–29], where σ is the Boltzmann constant, and δ, W and K_f represent the thickness of the flame, the width of XPS samples and the soot absorption coefficient, respectively. In the experiments, it was observed that the thickness of the flame was approximately the same to the thickness of XPS samples, which was 3 cm. If the thickness of the flame is assumed as a constant, i.e., 3 cm, the radiative heat flux of the flame can also be regarded as a constant value. Exposing to the flame, the temperature of the curtain wall increases and thus there is the radiative heat feedback from the curtain wall to the virgin PMMA. According to the Boltzmann law, the radiative heat feedback of the curtain wall can be expressed as $\dot{q}''_{fw} = F_{fw}\varepsilon\sigma T_{fw}^4$, where F_{fw}, ε and T_{fw} denote the view factor, the emissivity and the temperature of the curtain wall, respectively. F_{fw} and T_{fw} will be significantly influenced with the curtain wall coverage rate, which further affects the radiative heat feedback of the curtain wall. When the curtain wall is absent, $\dot{q}''_{fw} = 0$. The above analysis suggests that the variation of the radiative heat feedback of curtain wall determines the change in the flame spread rate.

Fig. 5 shows the flame spread rate under the coupling effect of structure factor and curtain wall coverage rate. The flame spread rate decreases first and then increases with the increase of coverage rate. This may be ascribed to two aspects. On the one hand, the increase of coverage rate inhibits the air entrainment in front of the flame, and thus the oxygen supply is restricted, which will reduce the combustion efficiency and inhibit flame spread. On the other hand, the increase of coverage rate strengthens the radiative heat feedback from curtain wall to the XPS surface, which will promote flame spread. When the coverage rate is less than 0.2, the former

Table 3
The fitted values of m and.n

α	β	m	n
1.0	0	3.33	0.8
	0.2	4.68	0.73
	0.4	4.29	0.76
	0.6	6.76	0.62
	0.8	4.07	0.75
1.2	0	13.96	0.48
	0.2	9.86	0.54
	0.4	8.14	0.59
	0.6	4.88	0.68
	0.8	6.62	0.61
1.4	0	12.4	0.52
	0.2	25.87	0.3
	0.4	2.87	0.84
	0.6	6.1	0.64
	0.8	5.36	0.68

dominates, and when the coverage rate is greater than 0.2, the latter plays a dominant role. Therefore, the flame spread rate decreases first and then increases.

Fig. 5 indicates that when the coverage rate is 0, the flame spread rate under different structure factors does not change obviously, which is consistent with the results of An et al. [18]. It can be seen from Eq. (3) that when the curtain wall coverage rate is 0, the heat flux received by the surface of the unburned material is only the radiative heat flux and convective heat flux of the flame, which are not correlated with the structure factor. When the coverage rate is greater than 0, the larger the structure factor, the larger the space inside the vertical channel, the more sufficient the oxygen supply, and the higher the combustion efficiency. Thus, the flame spread rate increases with the increasing structure factor.

In Fig. 6, performing linear fitting on the flame spread rate with a coverage rate of 0.2–0.8 and a structure factor of 1.0–1.4, the following equation can be obtained:

$$V_f = b\beta + c \tag{4}$$

where b and c are the fitting coefficients, and the detailed fitting coefficients are shown in Table 4.

The coefficients b and c are related to the structure factor. As shown in Table 4, the value of b increases with the increase of structure factor, while the value of c decreases as the structure factor increases. A linear function is used to correlate b and c with the structure factor, and the fitting equation is:

$$b = 1.2\alpha - 1.12 \tag{5}$$

$$c = -0.33\alpha + 0.8 \tag{6}$$

Substituting Equations (5) and (6) into Equation (4), we can obtain:

$$V_f = 1.2\alpha\beta - 0.33\alpha - 1.12\beta + 0.8 \tag{7}$$

Thus, the flame spread rate can be expressed as,

$$V_f = \begin{cases} 0.65 & 1.0 \le \alpha \le 1.4\ \beta = 0 \\ 1.2\alpha\beta - 0.33\alpha - 1.12\beta + 0.8 & 1.0 \le \alpha \le 1.4\ 0.2 \le \beta \le 0.8 \end{cases} \tag{8}$$

Equation (8) can be used to predict the flame spread rate under the coupling effect of structure factor and curtain wall coverage rate. Fig. 7 shows the comparison between the experimental results and predicted results of flame spread rate, and the prediction error is smaller than 10%. This demonstrates the reliability of the model established in this work.

4. Conclusions

In this paper, the combustion behavior of energy conservation materials (XPS) in vertical channel of building façade under the coupling effect of structure factors (α) and curtain wall coverage rate (β) was studied. XPS combustion characteristics including the temperature distribution, flame height, pyrolysis length and flame spread rate were measured and discussed. The fire safety of XPS in vertical channel under different structure factors and coverage rates were evaluated. The main conclusions are as follows:

For $\alpha = 1.0$, the average value of maximum temperatures 2 cm away from XPS surface ($\overline{T}_{max-2}$) decreases as β rises, while for $\alpha =$ 1.2 or 1.4, as β rises, the variation of $\overline{T}_{max-2}$ is not significant. In addition, as β rises, the change in average value of maximum temperatures in the center of vertical channel ($\overline{T}_{max-c}$) is also not obvious. With an increase in α, $\overline{T}_{max-2}$ first decreases and then increases, while $\overline{T}_{max-c}$ gradually decreases. The XPS flame in the vertical channel is turbulent. There is a correlation between the flame

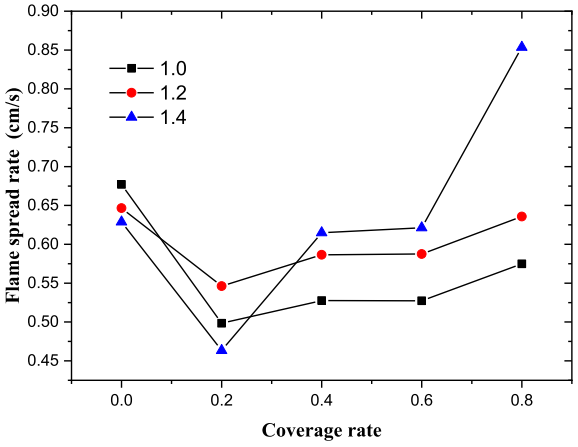

Fig. 5. Flame spread rate under different structure factors and coverage rates.

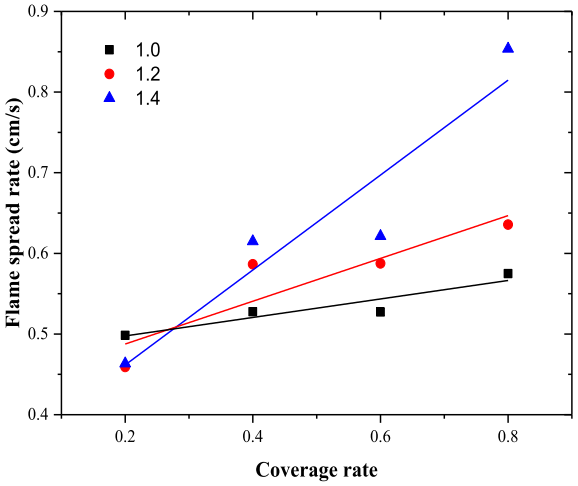

Fig. 6. Linear fitting of flame spread rate and coverage rate under different structure factors.

Table 4
Fitting values of variables *b* and.*c*

α	1.0	1.2	1.4
b	0.11	0.27	0.59
c	0.47	0.43	0.34

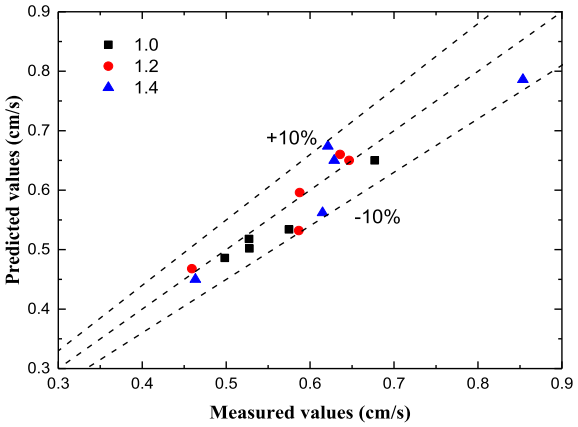

Fig. 7. Comparison between the experimental values and predicted results of flame spread rate.

height and pyrolysis length: $x_f = mx_p^n$, where *m* and *n* vary with the change in structure factor and coverage rate. The flame spread rate decreases first and then increases with the increase of coverage rate. When $0 \leq \beta < 0.2$, the restraining effect of the vertical channel on air entrainment dominates, while for $0.2 \leq \beta \leq 0.8$, the feedback heat feedback of the curtain wall plays a dominant role. When the curtain wall coverage rate is 0, the influence of structure factor on flame spread rate is not significant. The flame spread rate increases with the increasing structure factor when the curtain wall coverage rate changes from 0.2 to 0.8. A model is established to predict the flame spread rate under different coverage rates and structure factors. Compared with experimental results, the prediction error is smaller than 10%. Larger values of flame height and flame spread rate correspond to higher fire hazard.

This work is beneficial for fire risk assessment of building thermal insulation materials and optimal design of energy-saving curtain wall. The conclusions provide a reference for balancing fire protection and energy conservation of buildings. The results are helpful to build a sustainable and resilient city.

Author statement

Weiguang An: Conceptualization, Methodology, Funding acquisition, Formal analysis, Writing - Original Draft, Supervision,

Writing -Review & Editing, Validation.

Song Li: Investigation, Methodology, Writing - Original Draft, Data curation, Resources.

Xiangwei Yin: Investigation, Resources, Writing -Review & Editing.

Lujun Peng: Formal analysis, Resources, Validation.

Declaration of competing interest

The authors declare that they have no known competing financial interests or personal relationships that could have appeared to influence the work reported in this paper.

Acknowledgements

This research is supported by National Natural Science Foundation of China (No.51974298), National Key R&D Program of China (2016YFC0802907), Young Scientific and Technological Talents Supporting Project of Jiangsu Association for Science and Technology, China Postdoctoral Science Foundation (Nos. 2017T100421 and 2016M601917) and the Independent Research Project of State Key Laboratory of Coal Resources and Safe Mining, CUMT (SKLCRSM2020X03).

References

[1] Q.X. Meng, G.Q. Zhu, M.M. Yu, Z.H. Liang, Experimental study on upward flame spread characteristics of external thermal insulation material under the influence of porosity, Case Stud. Therm. Eng. 12 (2018) 365–373.
[2] Y.F. Huang, Y.F. Li, Experimental and theoretical research on the fire safety of a building insulation material via the ignition process study, Case Stud. Therm. Eng. 12 (2018) 77–84.
[3] Y. Zhou, R.W. Bu, L. Li, J.H. Sun, Heat transfer mechanism of concurrent flame spread over rigid polyurethane foam: effect of ambient pressure and inclined angle, Int. J. Therm. Sci. 155 (2020), 106403.
[4] R.W. Bu, Y. Zhou, C.G. Fan, Z.Y. Wang, Understanding the effects of inclination angle and fuel bed width on concurrent flame spread over discrete fuel arrays, Fuel 289 (2021), 119924.
[5] Z. Wang, W.M. Liang, M.L. Cai, Y.H. Tang, S. Li, W.G. An, G.Q. Zhu, Experimental study on flame spread over discrete extruded polystyrene foam with different fuel coverage rates, Case Stud. Therm. Eng. 17 (2020), 100577.
[6] S.F. Luo, Q.Y. Xie, L.J. Da, R. Qiu, Experimental study on thermal structure inside flame front with a melting layer for downward flame spread of XPS foam, J. Hazard Mater. 329 (2017) 30–37.
[7] S.F. Luo, Q.Y. Xie, R. Qiu, Melting and dripping flow behaviors on the downward flame spread of a wide XPS foam, Fire Technol. 55 (2018) 2055–2086.
[8] W.G. An, X.W. Yin, M.L. Cai, Y.H. Tang, Q. Li, X.M. Hu, Influence of U-shaped structure on upward flame spread and heat transfer behaviors of PMMA used in building thermal engineering, Case Stud. Therm. Eng. 22 (2020), 100794.
[9] G. Avinash, A. Kumar, V. Raghavan, Experimental analysis of diffusion flame spread along thin parallel solid fuel surfaces in a natural convective environment, Combust. Flame 165 (2016) 321–333.
[10] T. Matsuoka, K. Nakashima, T. Yamazaki, Y. Nakamura, Geometrical effects of a narrow channel on flame spread in an opposed flow, Combust. Sci. Technol. (190) (2018) 1–3.
[11] B. Comas, A. Carmona, T. Pujol, Experimental study of the channel effect on the flame spread over thin solid fuels, Fire Saf. J. 71 (2015) 162–173.
[12] W.G. An, X.W. Yin, M.L. Cai, Y.J. Gao, Influence of vertical channel on downward flame spread over extruded polystyrene foam, Int. J. Therm. Sci. 145 (2019), 105991.
[13] W.G. Yan, L. Jiang, W.G. An, Y. Zhou, J.H. Sun, Large scale experimental study on the fire hazard of buildings' U-shape façade wall geometry, J. Civ. Eng. Manag. (2017) 455–469.
[14] J.Y. Li, W.G. Yan, H.Y. Zhu, Q.S. Wang, J.H. Sun, Experimental study on the fire spread in high-rise building with U-shaped outside-façade structure, Fire Saf. Sci. 21 (2012) 167–173.
[15] H. Zhu, Y.J. Gao, R.L. Pan, B. Zhong, Spacing effects on downward flame spread over thin PMMA slabs, Case Stud. Therm. Eng. 13 (2019), 100370.
[16] S. Gao, G.Q. Zhu, Y.J. Gao, J.J. Zhou, Experimental study on width effects on downward flame spread over thin PMMA under limited distance condition, Case Stud. Therm. Eng. 13 (2019), 100382.
[17] W.G. An, T. Wang, K. Liang, Y.H. Tang, Z. Wang, Effects of interlayer distance and cable spacing on flame characteristics and fire hazard of multilayer cables in utility tunnel, Case Stud. Therm. Eng. 22 (2020), 100784.
[18] W.G. An, J.H. Sun, K.M. Liew, G.Q. Zhu, Effects of building concave structure on flame spread over extruded polystyrene thermal insulation material, Appl. Therm. Eng. 121 (2017) 802–809.
[19] J. Ji, Z.H. Gao, C.G. Fan, W. Zhong, J.H. Sun, A study of the effect of plug-holing and boundary layer separation on natural ventilation with vertical shaft in urban road tunnel fires, Int. J. Heat Mass Tran. 55 (2012) 6032–6041.
[20] F. Peng, D.M. Lai, Y. Zheng, L.Z. Yang, Effects of ceiling inclination on lateral flame spread over vertical Poly(methyl methacrylate) surface, Case Stud. Therm. Eng. 15 (2019), 100519.
[21] Q. Wang, L.H. Hu, X.Z. Zhang, X.L. Zhang, S.X. Lu, H. Ding, Turbulent jet diffusion flame length evolution with cross flows in a sub-pressure atmosphere, Energy Convers. Manag. 106 (2015) 703–708.
[22] W.G. An, J.H. Sun, K. Liew, G.Q. Zhu, Flammability and safety design of thermal insulation materials comprising PS foams and fire barrier materials, Mater. Des. 99 (2016) 500–508.
[23] J.G. Quintiere, The effects of angular orientation on flame spread over thin materials, Fire Saf. J. 36 (2001) 291–312.
[24] Y.H. Li, W.C. Kuo, The study of optimal parameters of oxygen-enriched combustion in fluidized bed with optimal torrefied woody waste, Int. J. Energy Res. 44 (2020) 7416–7434.
[25] W.G. An, Z. Wang, H.H. Xiao, J.H. Sun, K.M. Liew, Thermal and fire risk analysis of typical insulation material in a high elevation area: influence of sidewalls, dimension and pressure, Energy Convers. Manag. 88 (2014) 516–524.
[26] X. Chen, J.H. Liu, Z.H. Zhou, P. Li, T.N. Tian, D.C. Zhou, J. Wang, Experimental and theoretical analysis on lateral flame spread over inclined PMMA surface, Int. J. Heat Mass Tran. 91 (2015) 68–76.
[27] H.X. Wan, Z.H. Gao, J. Ji, J.H. Sun, Y.M. Zhang, K.Y. Li, Predicting heat fluxes received by horizontal targets from two buoyant turbulent diffusion flames of propane burning in still air, Combust. Flame 190 (2018) 260–269.
[28] Z. Lin, R.W. Bu, J.M. Zhao, Y. Zhou, Numerical investigation on fire-extinguishing performance using pulsed water mist in open and confined spaces, Case Stud. Therm. Eng. 13 (2019), 100402.
[29] R.W. Bu, Y. Zhou, L. Shi, C.G. Fan, Experimental study on combustion and flame spread characteristics in horizontal arrays of discrete fuels, Combust. Flame 225 (2021) 136–146.